

Synthesis of Nanocrystalline $\text{Ba}_{0.5}\text{Sr}_{0.5}\text{FeO}_{3-\delta}$ by Sol-gel Self-Combustion Method

F Fitriana, D Z Anjarwati, P S N Baity, and S Suasmo*

Dept. of Physics, Institut Teknologi Sepuluh Nopember Surabaya 60111, Indonesia

* Corresponding author: suasmo@its.ac.id

Abstract. Fuel cell is a one of device to convert chemical into proper electric energy, has some advantages including high efficiency, long term stability, fuel flexibility, environment friendly. To develop SOFC operates at intermediate temperature (500-700°C), it is necessary to figure out a cathode material capable of overcoming the low electrochemical reduction activity in oxygen at intermediate temperatures. $\text{Ba}_{0.5}\text{Sr}_{0.5}\text{FeO}_{3-\delta}$ (BSF) has mixed ionic and electronic conductivity properties (MIEC). A sol-gel self-combustion method was used to synthesize BSF due to easier preparation and produces excellent result (high homogeneity and high reactivity) powder. Two conditions were set up in different pH, namely 0-1 and 6-7. The self-combustion reaction occurred on heating up to 220 °C and produced yield ashes. To acquire the calcination condition, the temperature was carried out at 500, 700, 900, 1000, and 1100 °C for 6 hours. In this study, the phase formation, structure, and crystallite size of BSF was characterized by make use of X-ray diffraction (XRD) data. The results show that BSF has cubic perovskite structure with space group $pm3m$ (221), crystallite size 52 and 109 nm for pH 0-1 and 6-7 respectively.

Keywords: MIEC, perovskite, sol-gel self-combustion method.

1. Introduction

The perovskite oxide (ABO_3) is promising structure for MIEC material, due to BO_6 octahedra playing a role in ionic and electronic conductivity[1]. Cobalt-based perovskite oxides such as $\text{La}_{0.6}\text{Sr}_{0.4}\text{Co}_{0.2}\text{Fe}_{0.8}\text{O}_{3-\delta}$ and $\text{Ba}_{0.5}\text{Sr}_{0.5}\text{Co}_{0.8}\text{Fe}_{0.2}\text{O}_{3-\delta}$ have been widely used and reported to have high power density[2]. However, cobalt-based cathodes have some disadvantages: low chemical stability in reduced environments, large volume change due to cobalt ion spin transitions at the time of reduction, and reacts with zirconia-based electrolytes[3]. Therefore, from several options, the Fe (iron) -based cathode which has MIEC characteristic attracted much attention because of its catalytic activity similar to that of cobalt-grade perovskites, thermal stability and higher structure, low cost, and abundant presence[4,5]. Fe-based perovskite showed better stability than perovskite-based cobalt[5]. However, the Fe transition metal has several variables of oxidation and spin states, potentially affecting high catalytic activity and high resistance at the cathode[6]. $\text{BaFeO}_{3-\delta}$ has superior Oxygen Reaction Reduction (ORR) activity due to a high concentration of oxygen vacancies in their lattice structures[7]. In addition, Yin also reported that Sr doping provides the highest ratio between absorbed and surface oxygen[8] and a large ionic radius and a low valence state of Ba^{2+} are excellent in generating oxygen vacancies for oxygen transport[7].



Several methods are often used to synthesize SOFC electrodes that are solid state reaction[9], sol-gel[10,11], and self-combustion[7,12–16]. It is well known that solid state reaction process need a high temperature of calcination. The sol-gel method are complicated to do and the cost is high[14]. Combustion was chosen to synthesize perovskite $\text{BaFeO}_{3-\delta}$ due to easier in precursor preparation and produces excellent product with high homogeneity and high reactivity powder[12]. In addition, the combustion method produces a powdered product of nanocrystalline size[13].

In this study, we develop perovskite material based on $\text{Ba}_{0.5}\text{Sr}_{0.5}\text{FeO}_{3-\delta}$ as the basic material to develop new cathode material. We focus on the synthesis of $\text{Ba}_{0.5}\text{Sr}_{0.5}\text{FeO}_{3-\delta}$ powder by sol-gel self-combustion method. In this paper, we report the synthesis process, the phase formation, and crystal size which determined by X-ray diffraction.

2. Experimental

$\text{Ba}_{0.5}\text{Sr}_{0.5}\text{FeO}_{3-\delta}$ (BSF) powders were synthesized using sol-gel self-combustion method. Stoichiometric amount of $\text{Ba}(\text{NO}_3)_2$, $\text{Sr}(\text{NO}_3)_2$, and $\text{Fe}(\text{NO}_3)_3 \cdot 9\text{H}_2\text{O}$ were dissolved in deionized water at 30°C. And $\text{C}_6\text{H}_8\text{O}_7 \cdot 2\text{H}_2\text{O}$ solution were added under stirring to form an aqueous solution. The pH value was varied at 0-1 and 6-7 by adding ammonium solution. The mixed solution then heated at 100 °C and increased gradually at 150, 200, and 220 °C to obtain a dark solid precursor. The BSF powder was milled, and followed by calcination at 500, 700, 900, 1000, and 1100 °C for 6h in air to generate the desired perovskite oxide. The phase formation, structure and crystallite structure were determined by X-ray diffraction (XRD).

3. Results and Discussion

It was observed that all gels combusted into black powder of perovskite at 220°C. In sol-gel self-combustion method, metal ions react with COO^- in the solution to form metal-citrate complex. One of the factor that affect sol formation and its stability is pH value. Addition of ammonium solution for pH adjustment affect the dissociation of citric acid and metal complex formation as well. But, addition of ammonium solution should not precipitate and can destroy the balance of all reaction. Sol-gel self-combustion method of $\text{Ba}_{0.5}\text{Sr}_{0.5}\text{FeO}_{3-\delta}$ is based on the principle of oxidation and reduction, expressed by following reaction:

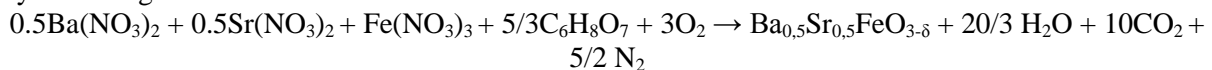


Table 1. Stability of sol and combustion degree with varied pH value.

	Sample Number	
	1	2
Ph	0-1	6-7
State of sol	Clear	Clear
Color of gel	Red-brown	Dark green
Combustion	Happened rapidly at 220 °C, some visible flame	Happened fast at 220 °C, no visible flame
Color of product	Brown and black powder	Brown and black powder

Figure 1 and 2 show the XRD pattern of $\text{Ba}_{0.5}\text{Sr}_{0.5}\text{FeO}_{3-\delta}$ at different temperature of calcination and varied pH value. The XRD pattern with pH 0-1 shows in Figure 1, which showed that the powder has formed crystallite after combustion with orthorhombic structure. The phase formation and composition of the powder shows in table 2.

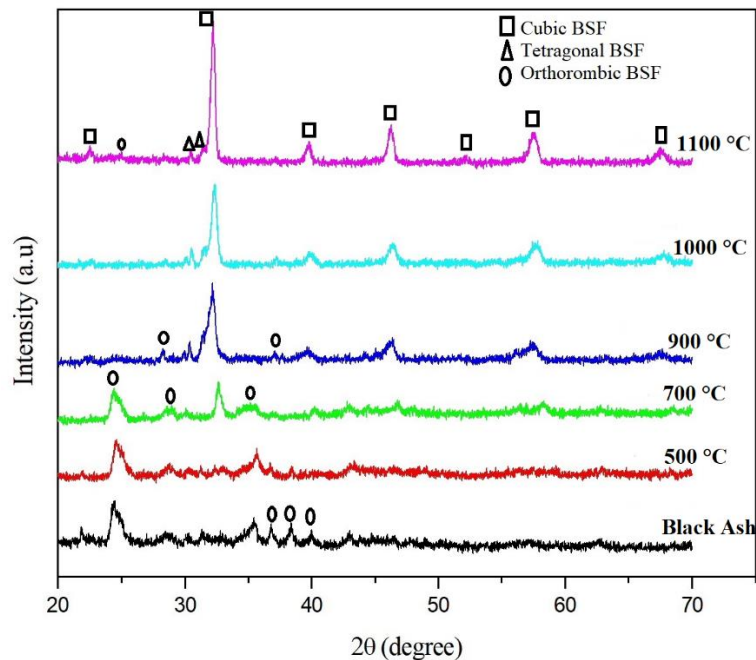


Figure 1. XRD Pattern of $\text{Ba}_{0.5}\text{Sr}_{0.5}\text{FeO}_{3-\delta}$ pH: 0-1 after 6 hours calcination at different temperature.

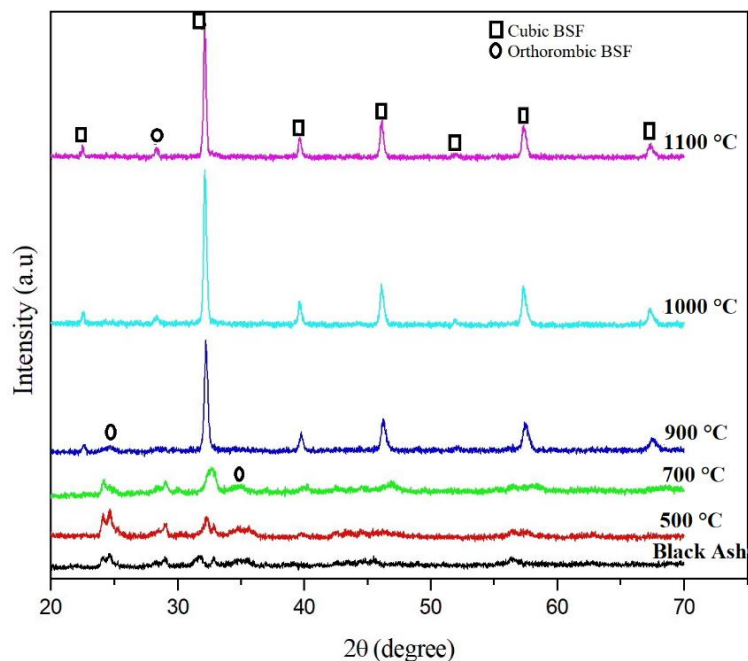


Figure 2. XRD Pattern of $\text{Ba}_{0.5}\text{Sr}_{0.5}\text{FeO}_{3-\delta}$ pH: 6-7 after 6 hours calcination at different temperature.

The phase transformation from orthorhombic to cubic occur at 900 °C based on XRD pattern for both pH value. XRD data shows the crystallization process at BSF with ammonium solution addition (pH: 6-7) faster than without ammonium solution (pH: 0-1). It is related to the influence of ammonium solution addition than can affect the dissociation of citric acid and metal complex formation. The cubic phase reaches 98,99 % at 900 °C for 6h when pH 7. This result is better than result reported by Toprak et.al [17] using oxalate co-precipitation. Another method also has been reported using solid

state reaction [18,19] but the calcined and sintered temperature were high. The result of Rietveld refinement method shows in Figure 3.

Table 2. Relative weight fraction of phases percent of $\text{Ba}_{0.5}\text{Sr}_{0.5}\text{FeO}_{3-\delta}$ (BSF) at different calcination temperature by Rietveld refinement.

Temperature	Relative weight fractions (%)		
	pH = 0-1		
	Cubic BSF (%)	Orthorhombic BSF (%)	Tetragonal BSF (%)
220 °C (Black ash)	-	100	-
500 °C	-	100	-
700°C	-	80.98	19.02
900°C	95.08	4.69	0.24
1000°C	96.96	1.95	1.09
1100°C	98.13	1.26	0.61
	pH = 6-7		
220 °C (Black ash)	-	100	-
500 °C	-	100	-
700°C	-	80.98	19.02
900°C	98.99	1.01	-
1000°C	96.73	3.27	-
1100°C	98.01	1.99	-

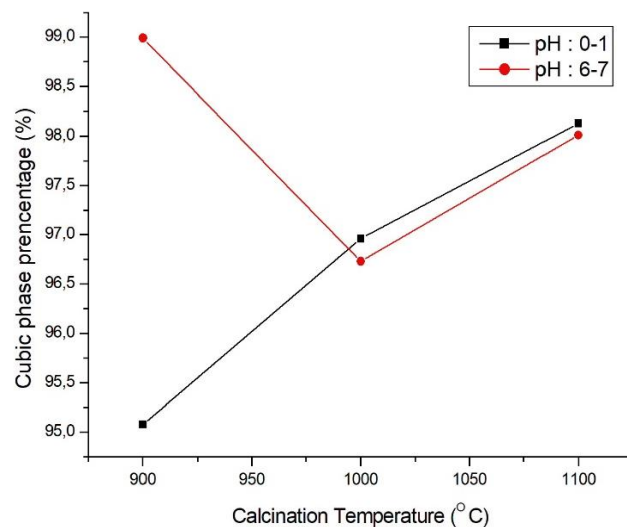
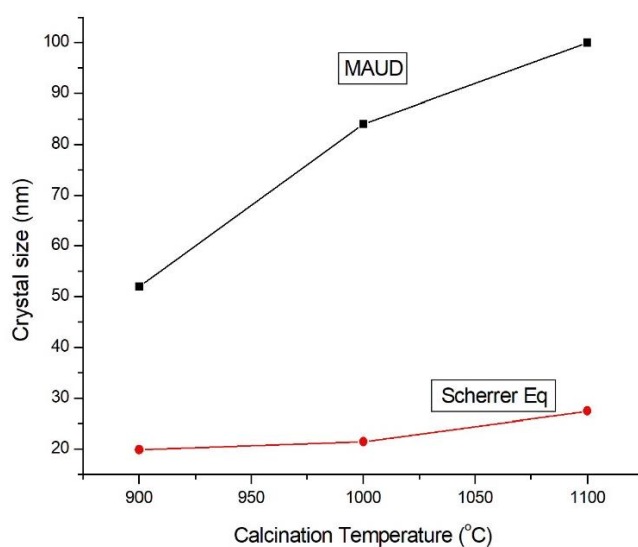


Figure 3. Cubic phase percentage related to the temperature of calcination for both pH value.

To analyze the change of lattice parameter in cubic, we used Rietveld refinement method. The result is shown on table 3. Based on Rietveld refinement result, the cubic phase (space group: $pm3m$ (221)), the average of lattice parameter is 3,91-3,93 (Å).

Table 3. Lattice Parameter of $\text{Ba}_{0.5}\text{Sr}_{0.5}\text{FeO}_{3-\delta}$ using Rietveld Refinement.

Calcination Temperature	Lattice Parameter (Å)		
	pH = 0-1		
	a (Å)	V (Å)	FoM
900 °C	3.9305 (3)	60.7222	Rbragg: 2,44; 5,77; 6,99 Rp: 7,71; Rwp: 9,78 Rexp: 7,53; GoF: 1,69
1000 °C	3.9143 (1)	59.9754	Rbrag: 1,96; 8,28; 9,06 Rp: 8,01; Rwp: 10,40 Rexp: 7,97; GoF: 1,70
1100 °C	3.9277 (7)	60.3622	Rbragg: 1,62; 4,51; 3,70 Rp: 7,03; Rwp: 8,93 Rexp: 7,41; GoF: 1,45
	pH = 6-7		
	a (Å)	V (Å)	FoM
900 °C	3.9224 (7)	60.3481	Rbragg: 2,71; 1,99 Rp: 6,40; Rwp: 8,12 Rexp: 7,53; GoF: 1,69
1000 °C	3.9304 (6)	60.7207	Rbragg: 1,56; 5,10 Rp: 6,55; Rwp: 8,19 Rexp: 7,08; GoF: 1,33
1100 °C	3.9266 (4)	60.5423	Rbragg: 1,64; 8,27 Rp: 7,08; Rwp: 9,22 Rexp: 7,81; GoF: 1,39

**Figure 4.** Crystal size related to the temperature of calcination at pH = 0-1.

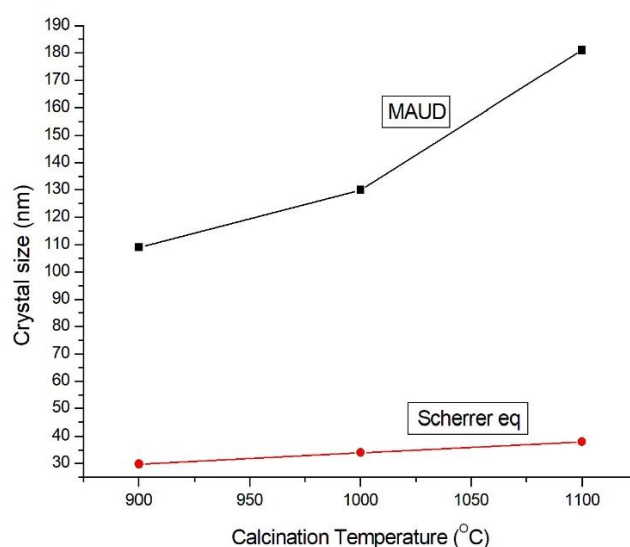


Figure 5. Crystal size related to the temperature of calcination at pH = 6-7.

The crystallite size was calculated by MAUD software and Scherrer equation. The result show that the crystal size is growing up by increasing temperature. The result is more accurate by using MAUD software than Scherrer equation.

4. Conclusion

Ba_{0.5}Sr_{0.5}FeO_{3-δ} cubic phase was obtained through sol-gel self-combustion method with calcination process at 900 °C for 6h for both pH value which varied. The smaller crystal size, 50-55 nm, achieve when the pH value is 0-1.

5. Reference

- [1] Kim D-Y, Miyoshi S, Tsuchiya T and Yamaguchi S 2014 Electronic Defect Formation in Fe-Doped BaZrO₃ Studied by X-Ray Absorption Spectroscopy *Chem. Mater.* **26** 927–34
- [2] Shan D, Gong Z, Wu Y, Miao L, Dong K and Liu W 2017 A novel BaCe_{0.5}Fe_{0.3}Bi_{0.2}O_{3-δ} perovskite-type cathode for proton-conducting solid oxide fuel cells *Ceram. Int.* **43** 3660–3
- [3] Wang J, Lam K Y, Saccoccio M, Gao Y, Chen D and Ciucci F 2016 Ca and In co-doped BaFeO_{3-δ} as a cobalt-free cathode material for intermediate-temperature solid oxide fuel cells *J. Power Sources* **324** 224–32
- [4] Zhang C and Zhao H 2012 A novel cobalt-free cathode material for proton-conducting solid oxide fuel cells *J. Mater. Chem.* **22** 18387–94
- [5] Wang J, Saccoccio M, Chen D, Gao Y, Chen C and Ciucci F 2015 The effect of A-site and B-site substitution on BaFeO_{3-δ}: An investigation as a cathode material for intermediate-temperature solid oxide fuel cells *J. Power Sources* **297** 511–8
- [6] Yang G, Shen J, Chen Y, Tadé M O and Shao Z 2015 Cobalt-free Ba_{0.5}Sr_{0.5}Fe_{0.8}Cu_{0.1}Ti_{0.1}O_{3-δ} as a bi-functional electrode material for solid oxide fuel cells *J. Power Sources* **298** 184–92
- [7] Dong F, Chen Y, Chen D and Shao Z 2014 Surprisingly High Activity for Oxygen Reduction Reaction of Selected Oxides Lacking Long Oxygen-Ion Diffusion Paths at Intermediate Temperatures: A Case Study of Cobalt-Free BaFeO_{3-δ} *ACS Appl. Mater. Interfaces* **6** 11180–9
- [8] Porras-Vazquez J M, Smith R I and Slater P R 2014 Investigation into the effect of Si doping on the cell symmetry and performance of Sr_{1-y}Ca_yFeO_{3-δ} SOFC cathode materials *J. Solid State Chem.* **213** 132–7
- [9] Chandratreya S S, Fulrath R M and Pask J A 1981 Reaction Mechanisms in the Formation of PZT Solid Solutions *J. Am. Ceram. Soc.* **64** 422–5
- [10] Budd K D, Dey S K and Payne D A 1985 Sol-Gel Processing of PbTiO₃, PbZrO₃, PZT, AND Plzt

Thin Films, *British Ceramic Proceedings*, **36** 107-121

- [11] Yi G and Sayer M 1996 An acetic acid/water based sol-gel PZT process I: Modification of Zr and Ti alkoxides with acetic acid *J. Sol-Gel Sci. Technol.* **6** 65-74
- [12] Schäfer J, Sigmund W, Roy S and Aldinger F 1997 Low temperature synthesis of ultrafine Pb(Zr, Ti)O₃ powder by sol-gel combustion *J. Mater. Res.* **12** 2518-21
- [13] Li Y, Xue L, Fan L and Yan Y 2009 The effect of citric acid to metal nitrates molar ratio on sol-gel combustion synthesis of nanocrystalline LaMnO₃ powders *J. Alloys Compd.* **478** 493-7
- [14] Guo R S, Wei Q T, Li H L and Wang F H 2006 Synthesis and properties of La_{0.7}Sr_{0.3}MnO₃ cathode by gel combustion *Mater. Lett.* **2** 261-5
- [15] Xiao S H, Jiang W F, Li L Y and Li X J 2007 Low-temperature auto-combustion synthesis and magnetic properties of cobalt ferrite nanopowder *Mater. Chem. Phys.* **106** 82-7
- [16] Gómez-Cuaspud J A and Vera-López E 2017 Synthesis and characterization of La_{0.8}Sr_{0.2}Ni_(1-x)Cr_xO₃ (x = 0.0, 0.2, 0.4, 0.6, 0.8, 1.0) system by the combustion method *Boletín la Soc. Española Cerámica y Vidr* **56**(6) 273-282
- [17] Toprak M S, Darab M, Syvertsen G E and Muhammed M 2010 Synthesis of nanostructured BSCF by oxalate co-precipitation - As potential cathode material for solid oxide fuels cells *Int. J. Hydrogen Energy* **35** 9448-54
- [18] Dong, F, Chen, Y, Ran, R, Chen, D, Tadé, M.O, Liu, S, Shao, Z 2013 BaNb_{0.05}Fe_{0.95}O_{3-δ} as a new oxygen reduction electrocatalyst for intermediate temperature solid oxide fuel cells *J. Mater. Chem. A* **1**(34) 9781-9791
- [19] Zhu M, Cai Z, Xia T, Li Q, Huo L and Zhao H 2016 Cobalt-free perovskite BaFe_{0.85}Cu_{0.15}O_{3-δ} cathode material for intermediate-temperature solid oxide fuel cells *Int. J. Hydrogen Energy* **41**(8) 4784-4791